AIAA JOURNAL
Vol. 31, No. 1, January 1993

Effect of Sidewall Suction on Flow in Two-Dimensional Wind Tunnels

Richard W. Barnwell*
NASA Langley Research Center, Hampton, Virginia 23681

A closed-form analysis of flow in a two-dimensional subsonic wind tunnel that uses sidewall suction around the model to reduce sidewall boundary-layer effects is presented. The model problem that is treated involves a flat plate airfoil in a tunnel with a suction window shaped to permit an analytic solution. This solution shows that the lift coefficient depends explicitly on the porosity parameter of the suction window and implicitly on the suction pressure differential. For a given sidewall displacement thickness, the lift coefficient increases as the suction-window porosity decreases.

Introduction

A SIMPLE analysis of the interaction of an airfoil model pressure field with the boundary layer on the solid wind-tunnel sidewall was presented by Barnwell in Ref. 1 and refined in Ref. 2. It was shown that this interaction in two-dimensional wind tunnels is mathematically similar to the effect of compressibility. This similarity rule was used to derive a modified form of the Prandtl-Glauert rule, which was validated by comparison with the experimental data of Bernard-Guelle.[3] Sewall[4] extended the analysis of the sidewall boundary-layer effect in two-dimensional wind tunnels to the transonic regime by developing a modified form of the von Karman rule and presented experimental data that validated these theoretical results. The results of Barnwell and Sewall for two-dimensional flow, which are summarized in Ref. 5, apply in the limit of small aspect ratio. Murthy[6] employed the wavy wall concept to account for aspect-ratio effects. A qualitative experimental study of solid sidewall boundary-layer effects was conducted recently by Su.[7]

Suction across porous plates has been used to control sidewall boundary-layer effects in some wind tunnels. For example, the control of sidewall boundary-layer growth with suction on large plates upstream of the model is described in Ref. 3, and the reduction of adverse effects with suction on porous windows at the model station is discussed in Ref. 8. The purpose of this article is to present an analysis of the effects of sidewall suction at the model station on the performance characteristics of the airfoil being tested. This analysis is an extension of a very limited analysis of the problem presented in Ref. 1. To the author's knowledge, there is no experimental data applicable to the particular problem discussed here.

The model problem that is treated concerns subsonic flow past slender ellipses; this family of bodies includes the flat plate. First, the theory of Refs. 1 and 2 is used to account for sidewall boundary-layer effects. Then the Prandtl-Glauert rule as modified in Refs. 1 and 2 is used to map the compressible airfoil problem to an incompressible airfoil problem. The Joukowski transformation is then used to map the airfoil problem to the problem of flow about a circular cylinder. It is assumed 1) that the outer edge of the porous plate in the transform plane is a circle that is concentric to the circular cylinder and 2) that the flow within the porous plate is laminar (the porous material of which the plate is composed is fine enough that the fluid flowing through it is always within the laminar sublayer of one of the fibers or grains of the material). Closed form solutions are obtained for asymptotically small values of the porosity coefficient. The results for the flat plate show that the lift on the plate is an indirect function of the pressure difference across the porous window and an explicit function of the window porosity.

Derivation of Basic Equations

Consider steady, isentropic, small-perturbation flow in a nominally two-dimensional airfoil wind tunnel. Let the Cartesian coordinates in the freestream, normal, and spanwise directions be x, y, and z, and let the velocity components be u, v, and w as shown in Fig. 1. The tunnel width and sidewall boundary-layer displacement thickness are b and δ^*, respectively. To the lowest order, the spanwise velocity component in this tunnel varies linearly as

$$w = -\frac{2uz}{b}\frac{\partial \delta^*}{\partial x}$$

As a result, the continuity equation can be written as

$$(1 - M^2)\frac{\partial u}{\partial x} + \frac{\partial v}{\partial y} = -\frac{\partial w}{\partial z} = \frac{2u}{b}\frac{\partial \delta^*}{\partial x} \tag{1}$$

where M is the Mach number.

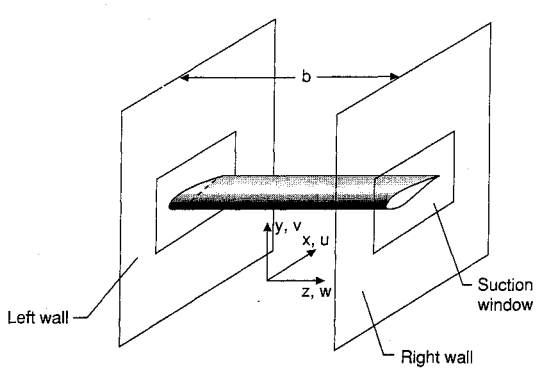

Fig. 1 Sketch of airfoil model and tunnel sidewalls with coordinate system used.

Presented as Paper 84-0242 at the AIAA 22nd Aerospace Sciences Meeting, Reno, NV, Jan. 9-12, 1984; received Dec. 20, 1991; revision received May 20, 1992; accepted for publication July 6, 1992.

*Associate Chief, Space Systems Division. Fellow AIAA.

The dynamics of the sidewall boundary layer are modeled with the von Karman momentum integral, which can be written as

$$\frac{\partial \delta^*}{\partial x} = -\frac{\delta^*}{u}(2 + H - M^2)\frac{\partial u}{\partial x} + \frac{\delta^*}{H}\frac{\partial H}{\partial x} + \frac{H\tau_w}{\rho u^2} + \frac{Hw_o}{u} \quad (2)$$

where ρ is the density, H and τ_w the sidewall boundary-layer shape factor and surface shearing stress, and w_o the suction velocity at the sidewall surface. This equation can be simplified because the sidewall boundary layer in most airfoil wind tunnels can be approximated as a flat-plate boundary layer with a large Reynolds number and an equivalent length at the model station of the order of $\delta^*/(\tau_w/\rho u^2)$. In general, the model chord c is much smaller than this boundary-layer equivalent length so that the inequality

$$\frac{\tau_w}{\rho u^2} \ll \frac{\delta^*}{c} \quad (3)$$

applies and, as a result, the next to last term in Eq. (2) can be neglected in the first approximation. As shown in Refs. 2, 4, and 5, the gradient of the shape factor can be approximated as

$$\frac{\partial H}{\partial x} = \frac{(H-1)(H+1)}{u}\frac{\partial u}{\partial x} \quad (4)$$

With inequality Eq. (3) and Eq. (4), Eq. (2) can be approximated as

$$\frac{\partial \delta^*}{\partial x} = -\frac{\delta^*}{u}\left(2 + \frac{1}{H} - M^2\right)\frac{\partial u}{\partial x} + \frac{Hw_o}{u} \quad (5)$$

With Eq. (5), Eq. (1) can be written as

$$\left[1 - M^2 + \left(2 + \frac{1}{H} - M^2\right)\frac{2\delta^*}{b}\right]\frac{\partial u}{\partial x} + \frac{\partial v}{\partial y} = \frac{2Hw_o}{b} \quad (6)$$

It is assumed that the sidewall boundary layers are attached and that the flat-plate-type growth of this boundary layer at the model station is small. Therefore, the shape factor H and the displacement thickness δ^* of the sidewall boundary layer near the model station can be approximated to the lowest order by the values at the model station in the empty tunnel. For subsonic flow the Mach number M can be equated to the freestream value M_∞ so that Eq. (6) can be written as

$$\bar{\beta}^2\frac{\partial u}{\partial x} + \frac{\partial v}{\partial y} = \frac{2Hw_o}{b} \quad (7)$$

where

$$\bar{\beta} = \sqrt{1 - M_\infty^2 + \left(2 + \frac{1}{H} - M_\infty^2\right)\frac{2\delta^*}{b}} \quad (8)$$

This equation and the irrotational condition

$$\frac{\partial u}{\partial y} - \frac{\partial v}{\partial x} = 0$$

completely govern the flow.

If the sidewall is solid so that $w_o = 0$, the normal-force coefficient $\bar{C}_n$ in a wind tunnel with a sidewall boundary layer is related to the normal-force coefficient C_n in the same wind tunnel without a sidewall boundary layer by the modified Prandtl-Glauert rule

$$\bar{\beta}\bar{C}_n = \beta C_n$$

where

$$\beta = \sqrt{1 - M_\infty^2}$$

As discussed in Refs. 1 and 2, this similarity rule shows that the lift is reduced at a given angle of attack by the presence of a sidewall boundary layer.

Physics of Sidewall Suction

Now consider a wind tunnel with suction over the sidewall around the model. It is assumed that the sidewall can be approximated as a porous plate and that the plenum pressure p_p behind the plate is the same everywhere. Thus, the sidewall suction velocity can be written as

$$\frac{\Delta p}{\rho_\infty u_\infty^2} = \frac{p - p_p}{\rho_\infty u_\infty^2} = \frac{1}{P}\left(-\frac{w_o}{u_\infty}\right)^n \quad (9)$$

where P is a nondimensional porosity constant, p the local tunnel pressure, ρ_∞ and u_∞ the free-stream density and velocity, and n a constant that varies between 1 and 2. For the value $n = 2$ the flow within the plate is turbulent, and for $n = 1$ it is laminar. As discussed in the introduction, laminar flow occurs within the plate when the fluid is always within the laminar sublayer of the particles or fibers of the porous material.

Actual values of n for porous plates in use generally lie between 1 and 2, as illustrated in Fig. 2. Note that the porosity coefficient decreases as the exponent n approaches 1.

In this article the value $n = 1$ will be used in Eq. (9). This value is physically realistic in many cases, and it causes Eq. (7) to be linear. With the small-disturbance approximation, the pressure can be written as

$$p = p_\infty + \rho_\infty u_\infty(u_\infty - u)$$

where p_∞ is the freestream pressure. As a result, Eq. (9) can be written as

$$w_o = P\left(u - u_\infty - \frac{p_\infty - p_p}{\rho_\infty u_\infty}\right) \quad (10)$$

With Eq. (10), Eq. (7) can be written as

$$\bar{\beta}^2\frac{\partial u}{\partial x} + \frac{\partial v}{\partial y} = \frac{2HP}{b}\left(u - u_\infty - \frac{p_\infty - p_p}{\rho_\infty u_\infty}\right) \quad (11)$$

This equation contains two parameters related to the sidewall suction: a porosity parameter that is proportional to P and a plenum-pressure parameter that depends on p_p. As shown in Ref. 1, the effects of these parameters on the lift and thickness solutions can be identified. Assume that the airfoil boundary conditions are applied along the x axis, and let the u and v velocity components be written as

$$u = u_l + u_t$$

$$v = v_l + v_t$$

where the subscripts l and t denote the lift and thickness solutions, which are odd and even solutions, respectively, of the coordinate y.

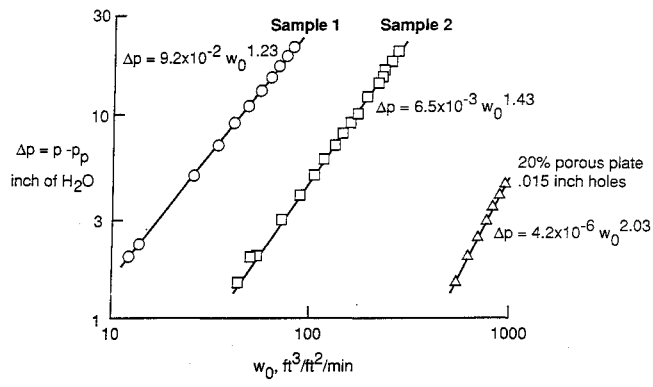

Fig. 2 Porosity characteristics of several materials.

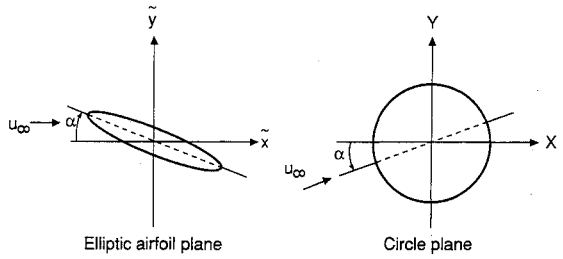

Fig. 3 Incompressible Joukowski transformation.

The governing equations for the lift and thickness solutions are obtained from Eq. (11) as

$$\bar{\beta}^2 \frac{\partial u_l}{\partial x} + \frac{\partial v_l}{\partial y} = \frac{2HP}{b} u_l$$

$$\bar{\beta}^2 \frac{\partial u_t}{\partial x} + \frac{\partial v_t}{\partial y} = \frac{2HP}{b}\left(u_t - u_\infty - \frac{p_\infty - p_p}{\rho_\infty u_\infty}\right)$$

It is seen that the thickness solution depends explicitly on both parameters, but the lift solution depends explicitly only on the porosity parameter P. It follows that the lift solution is affected by the plenum pressure only in the way that the displacement thickness δ^* in $\bar{\beta}$ is affected.

Prandtl-Glauert Transformation

This transformation is used to transform from the compressible airfoil plane to an incompressible airfoil plane. Define nondimensional coordinates and velocity components as

$$\tilde{x} = x/c \qquad \tilde{y} = \bar{\beta} y/c$$

$$\tilde{u} = u/u_\infty \qquad \tilde{v} = v/\bar{\beta} u_\infty$$

Equation (11) is written as

$$\frac{\partial \tilde{u}}{\partial \tilde{x}} + \frac{\partial \tilde{v}}{\partial \tilde{y}} = \epsilon(\tilde{u} - 1 - \hat{u}) \tag{12}$$

where

$$\epsilon = \frac{2HP}{\bar{\beta}^2}\frac{c}{b}$$

and

$$\hat{u} = \frac{p_\infty - p_p}{\rho_\infty u_\infty^2}$$

Joukowski Transformation

This transformation is used to transform from the incompressible airfoil plane to the incompressible circle plane. Let Φ be defined as the nondimensional, incompressible velocity potential. The complex variable in the incompressible airfoil plane is

$$\zeta = \tilde{x} + i\tilde{y}$$

Equation (12) can be written as

$$4\frac{\partial^2 \Phi}{\partial \zeta\, \partial \zeta^*} = \epsilon\left[\frac{\partial \Phi}{\partial \zeta} + \frac{\partial \Phi}{\partial \zeta^*} - (1 + \hat{u})\right]$$

where ζ^* is the complex conjugate of ζ.

Now consider the transformation depicted in Fig. 3. The elliptic airfoils have major and minor axes of a and b, respectively, and the circle has the radius

$$r_b = \frac{a + b}{2}$$

The complex variable in the circle plane is

$$Z = X + iY = re^{i\theta}$$

and the transformation from the airfoil plane to the circle plane is

$$Z = \tfrac{1}{2}(\zeta e^{i\alpha} + \sqrt{\zeta^2 e^{2i\alpha} - C^2})$$

or

$$\zeta = e^{-i\alpha}\left(Z + \frac{C^2}{4Z}\right)$$

where

$$C^2 = a^2 - b^2$$

Note that the freestream is aligned with the $\tilde{x}$ axis in the airfoil plane and makes an angle α with the X axis in the circle plane. The transformed governing equation is

$$4\frac{\partial^2 \Phi}{\partial Z\, \partial Z^*} = \epsilon\left[\frac{d\zeta^*}{dZ^*}\frac{\partial \Phi}{\partial Z} + \frac{d\zeta}{dZ}\frac{\partial \Phi}{\partial Z^*} - \frac{d\zeta}{dZ}\frac{d\zeta^*}{dZ^*}(1 + \hat{u})\right] \tag{13}$$

Let the velocity components in the r and θ directions in the circle plane be U and V. Eq. (13) can be written as

$$\frac{\partial U}{\partial r} + \frac{U}{r} + \frac{1}{r}\frac{\partial V}{\partial \theta} = \epsilon\left\{U\cos(\theta - \alpha) - V\sin(\theta - \alpha)\right.$$

$$-\frac{C^2}{4r^2}[U\cos(\theta + \alpha) + V\sin(\theta + \alpha)]$$

$$\left.-(1 + \hat{u})\left(1 - \frac{C^2}{2r^2}\cos 2\theta + \frac{C^4}{16r^4}\right)\right\} \tag{14}$$

The irrotational condition is

$$\frac{\partial V}{\partial r} + \frac{V}{r} - \frac{1}{r}\frac{\partial U}{\partial \theta} = 0 \tag{15}$$

Circle Plane Solution

In this article Eqs. (14) and (15) are solved for small values of the porosity parameter ϵ. The velocity components U and V are written as

$$U = U_o + \epsilon U_1$$

$$V = V_o + \epsilon V_1$$

It is assumed that the suction window has a circular shape in the circle plane that is concentric to the circular body, as shown in Fig. 4.

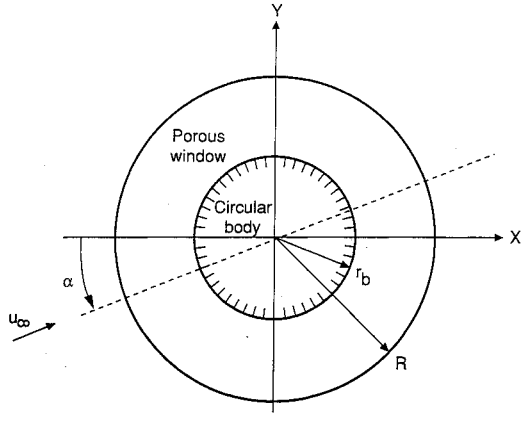

Fig. 4 Body and suction window in circle plane.

The zero-order solution is the well-known solution for flow past a circular cylinder, which is written as

$$U_o = \left(1 - \frac{r_b^2}{r^2}\right) \cos(\theta - \alpha)$$

$$V_o = -\left(1 + \frac{r_b^2}{r^2}\right) \sin(\theta - \alpha) - \frac{\Gamma}{2\pi r}$$

where Γ is the circulation.

The governing equations for the first-order problem in the region of the porous plate, where $r_b \le r \le R$, are

$$\frac{\partial U_1}{\partial r} + \frac{U_1}{r} + \frac{1}{r}\frac{\partial V_1}{\partial \theta} = -\frac{r_b^2}{r^2}\cos[2(\theta - \alpha)] + \frac{C^2 r_b^2}{4r^4}\cos 2\alpha + \frac{C^2}{4r^2}\cos 2\theta - \frac{C^4}{16r^4} - \left(1 - \frac{C^2}{2r^2}\cos 2\theta + \frac{C^4}{16r^4}\right)\hat{u} + \frac{\Gamma}{2\pi r}\sin(\theta - \alpha) + \frac{\Gamma C^2}{8\pi r^3}\sin(\theta + \alpha) \quad (16)$$

and

$$\frac{\partial V_1}{\partial r} + \frac{V_1}{r} - \frac{1}{r}\frac{\partial U_1}{\partial \theta} = 0$$

Beyond the porous plate, where $r > R$, the right side of Eq. (16) is zero. By differentiation and substitution, equations for U_1 and V_1 can be obtained as

$$r^2\frac{\partial^2 U_1}{\partial r^2} + 3r\frac{\partial U_1}{\partial r} + U_1 + \frac{\partial^2 U_1}{\partial \theta^2} = -\frac{C^2 r_b^2}{2r^3}\cos 2\alpha + \frac{C^4}{8r^3}(1 + \hat{u}) - 2r\hat{u} + \frac{\Gamma}{2\pi}\sin(\theta - \alpha) - \frac{\Gamma C^2}{8\pi r^2}\sin(\theta + \alpha) \quad (17)$$

$$r^2\frac{\partial^2 V_1}{\partial r^2} + 3r\frac{\partial V_1}{\partial r} + V_1 + \frac{\partial^2 V_1}{\partial \theta^2} = 2\frac{r_b^2}{r^2}\sin[2(\theta - \alpha)] - \frac{C^2}{2r}(1 + 2\hat{u})\sin 2\theta + \frac{\Gamma}{2\pi}\cos(\theta - \alpha) + \frac{\Gamma C^2}{8\pi r^2}\cos(\theta + \alpha) \quad (18)$$

Now let the coordinate

$$\eta = \ell n\, r$$

be defined. Equations (17) and (18) can be written as

$$\frac{\partial^2 U_1}{\partial \eta^2} + 2\frac{\partial U_1}{\partial \eta} + U_1 + \frac{\partial^2 U_1}{\partial \theta^2} = -\frac{C^2}{2}r_b^2 e^{-3\eta}\cos 2\alpha + \frac{C^4}{8}(1 + \hat{u})e^{-3\eta} - 2\hat{u}e^{\eta} + \frac{\Gamma}{2\pi}\sin(\theta - \alpha) - \frac{\Gamma}{8\pi}C^2 e^{-2\eta}\sin(\theta + \alpha) \quad (19)$$

$$\frac{\partial^2 V_1}{\partial \eta^2} + 2\frac{\partial V_1}{\partial \eta} + V_1 + \frac{\partial^2 V_1}{\partial \theta^2} = 2r_b^2 e^{-2\eta}\sin[2(\theta - \alpha)] - \frac{C^2}{2}(1 + 2\hat{u})e^{-\eta}\sin 2\theta + \frac{\Gamma}{2\pi}\cos(\theta - \alpha) + \frac{\Gamma}{8\pi}C^2 e^{-2\eta}\cos(\theta + \alpha) \quad (20)$$

The most general complementary solution to Eq. (19) is

$$U_{1,c} = Ae^{-\eta} + B\eta e^{-\eta} + \left[Ge^{(m-1)\eta} + \frac{D}{e^{(m+1)\eta}}\right]\cos m\theta + \left[Ee^{(m-1)\eta} + \frac{F}{e^{(m+1)\eta}}\right]\sin m\theta \quad (21)$$

where m is a positive integer. Although the solution may contain any number of harmonics of θ, the present solution contains only terms with $m = 1$ for the lift solution and $m = 2$ for the thickness solution. The complementary solution for V_1 is of the same form as Eq. (21).

The particular solutions to Eqs. (19) and (20) are

$$U_{1,p} = \frac{C^2}{8}\left[r_b^2\cos 2\alpha - \frac{C^2}{4}(1 + \hat{u})\right]e^{-3\eta} - \frac{\hat{u}}{2}e^{\eta} + \frac{\Gamma}{4\pi}\sin(\theta - \alpha) - \frac{\Gamma}{16\pi}C^2\eta e^{-2\eta}\sin(\theta + \alpha)$$

and

$$V_{1,p} = -\frac{r_b^2}{2}e^{-\eta}\sin[2(\theta - \alpha)] + \frac{C^2}{8}(1 + 2\hat{u})e^{-\eta}\sin 2\theta + \frac{\Gamma}{4\pi}\cos(\theta - \alpha) - \frac{\Gamma}{16\pi}C^2\eta e^{-2\eta}\cos(\theta + \alpha)$$

These particular solutions pertain only near the porous window where $r_b \le r \le R$.

Beyond the window, where $r > R$, the solution is composed of complementary-solution terms that vanish for large values of r. The solutions near the window are termed $U_{1,\text{outer}}$ and $V_{1,\text{outer}}$. Near the window, where $r_b \le r \le R$, the solution includes the particular solution and various complementary-solution terms, which are not necessarily the same terms appearing in the outer solution. The solutions near the window are termed $U_{1,\text{inner}}$ and $V_{1,\text{inner}}$.

The boundary conditions for this problem are

$$U_{1,\text{inner}} = U_{1,\text{outer}} \quad \text{for} \quad r = R$$

$$V_{1,\text{inner}} = V_{1,\text{outer}} \quad \text{for} \quad r = R$$

$$U_{1,\text{inner}} = 0 \quad \text{for} \quad r = r_b$$

With these boundary conditions the solution near the window ($r_b \le r \le R$) is found to be

$$U_1 = -\frac{\hat{u}}{2r}(r^2 - r_b^2) - \frac{C^2(r^2 - r_b^2)}{8r_b^2 r^3}\left[r_b^2\cos 2\alpha - \frac{C^2}{4}(1 + \hat{u})\right] - \frac{(r^4 - r_b^4)}{4R^2 r^3}\left\{r_b^2\cos[2(\alpha - \theta)] - \frac{C^2}{4}(1 + \hat{u})\cos 2\theta\right\} - \frac{\Gamma}{4\pi}\left\{\left[\ell n\left(\frac{R}{r}\right) - \frac{r_b^2}{r^2}\ell n\left(\frac{R}{r_b}\right)\right]\sin(\theta - \alpha) - \frac{C^2}{4r^2}\ell n\left(\frac{r}{r_b}\right)\sin(\theta + \alpha)\right\} \quad (22)$$

$$V_1 = \frac{1}{2r}\left[\frac{(r^4 + r_b^4)}{2R^2 r^2} - 1\right]\left\{r_b^2\sin[2(\theta - \alpha)] - \frac{C^2}{4}(1 + 2\hat{u})\sin 2\theta\right\} - \frac{\Gamma}{4\pi}\left\{\left[\ell n\left(\frac{R}{r}\right) + \frac{r_b^2}{r^2}\ell n\left(\frac{R}{r_b}\right)\right]\cos(\theta - \alpha) + \frac{C^2}{4r^2}\ell n\left(\frac{r}{r_b}\right)\cos(\theta + \alpha)\right\} \quad (23)$$

Beyond the window, where $r > R$, the solution is

$$U_1 = -\hat{u}\frac{(R^2 - r_b^2)}{2r} - \frac{C^2(R^2 - r_b^2)}{8R^2 r_b^2 r}\left[r_b^2\cos 2\alpha - \frac{C^2}{4}(1 + \hat{u})\right] - \frac{(R^2 - r_b^2)}{4R^2 r^3}\left\{r_b^2\cos[2(\theta - \alpha)] - \frac{C^2}{4}(1 + 2\hat{u})\cos 2\theta\right\} - \frac{\Gamma}{4\pi r^2}\ell n\left(\frac{R}{r_b}\right)\left[r_b^2\sin(\theta - \alpha) - \frac{C^2}{4}\sin(\theta + \alpha)\right] \quad (24)$$

$$V_1 = -\frac{(R^2 - r_b^2)}{4R^2 r^3}\left\{r_b^2 \sin[2(\theta - \alpha)] - \frac{C^2}{4}(1 + 2\hat{u}) \sin 2\theta\right\}$$
$$-\frac{\Gamma}{4\pi r^2}\left[r_b^2 \cos(\theta - \alpha) + \frac{C^2}{4}\cos(\theta + \alpha)\right] \quad (25)$$

Note that all lengths in Eqs. (22) to (25) are made nondimensional with the airfoil chord c.

Kutta Condition for Flat Plate

For a flat plate the minor and major axes are $b = 0$ and $a = 2r_b$, respectively. Also, the quantity C and the airfoil chord c have the values $2r_b$ and $4r_b$, respectively. Because all lengths are made nondimensional with the chord c, the nondimensional radius r_b has the value ¼.

The streamwise component of velocity in the incompressible airfoil plane is

$$\tilde{u} = \frac{\partial \Phi}{\partial \tilde{x}} = \frac{dZ}{d\zeta}\frac{\partial \Phi}{\partial Z} + \frac{dZ^*}{d\zeta^*}\frac{\partial \Phi}{\partial Z^*} \quad (26)$$

At the surface of the plate, Eq. (26) can be written as

$$\tilde{u} = -\frac{\cos \alpha}{2 \sin \theta} V \quad (27)$$

The traditional Kutta condition is obtained from the zero order form of Eq. (27). The circulation is related to the incompressible airfoil lift coefficient C_L by the equation

$$\Gamma = \frac{C_L c}{2}$$

Assume that the angle of attack is of the form

$$\alpha = \alpha_o + \epsilon\alpha_1 \quad (28)$$

To the lowest order, Eq. (27) is written as

$$\tilde{u}_o = \frac{\cos \alpha_o}{\sin \theta}\left(\sin \theta \cos \alpha_o - \cos \theta \sin \alpha_o + \frac{C_L}{2\pi}\right)$$

In order for the solution at the trailing edge ($\theta = 0$) to be finite, the Kutta condition

$$C_L = 2\pi \sin \alpha_o \quad (29)$$

is imposed.

The Kutta condition for the first-order solution determines the effect of porosity on the incompressible airfoil lift coefficient. With Eq. (28), the function $\sin \alpha$ can be written as

$$\sin \alpha = \sin \alpha_o + \epsilon\alpha_1 \cos \alpha_o \quad (30)$$

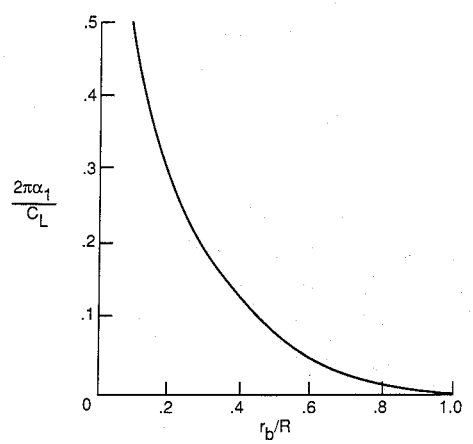

Fig. 5 Dependence of first-order Kutta condition parameter on suction window size.

Therefore, the first-order solution is

$$\tilde{u}_1 = -\frac{\cos \alpha}{2 \sin \theta}\left[2\alpha_1 \cos \theta \cos \alpha_o + r_b\left(1 - \frac{r_b^2}{R^2}\right)(\sin^2\alpha_o + \hat{u}) \sin 2\theta + r_b\left(1 - \frac{r_b^2}{R^2}\right) \sin \alpha_o \cos \alpha_o (\cos^2\theta - \sin^2\theta) - r_b \frac{C_L}{\pi} \sin \alpha_o \ell n \left(\frac{R}{r_b}\right) \sin \theta - r_b \frac{C_L}{\pi} \cos \alpha_o \ell n \left(\frac{R}{r_b}\right) \cos \theta\right]$$

In order for $\tilde{u}_1$ to be finite at the trailing edge ($\theta = 0$), the condition

$$\alpha_1 = r_b\left[\ell n \left(\frac{R}{r_b}\right) - \frac{1}{2}\left(1 - \frac{r_b^2}{R^2}\right)\right] \sin \alpha_o \quad (31)$$

must be imposed. The function of the ratio r_b/R in Eq. (31) is positive definite for all values in the range $0 \le r_b/R \le 1$, as shown in Fig. 5.

Discussion of Results

The physical angle of attack in the incompressible airfoil plane is α. With Eqs. (29) and (30), the function $\sin \alpha$ can be related to the lift coefficient to the first order in ϵ as

$$C_L = 2\pi\left\{1 - \frac{\epsilon}{4}\cos \alpha\left[\ell n \left(\frac{R}{r_b}\right) - \frac{1}{2}\left(1 - \frac{r_b^2}{R^2}\right)\right]\right\} \sin \alpha$$

Note that for small angles of attack, $\sin \alpha$ can be approximated by α.

Let the angle of attack in the compressible airfoil plane be denoted as α_c. With the Prandtl-Glauert rule it can be shown that, for the same lift coefficient, the angles of attack of the flat plate in the incompressible and compressible airfoil planes are related as

$$\alpha = \frac{\alpha_c}{\bar{\beta}}$$

It follows that the lift coefficient for the flat plate in compressible flow can be written as

$$\bar{C}_L = \frac{2\pi\alpha_c}{\bar{\beta}}\left\{1 - \frac{HP}{2\bar{\beta}^2}\frac{c}{b}\left[\ell n \left(\frac{R}{r_b}\right) - \frac{1}{2}\left(1 - \frac{r_b^2}{R^2}\right)\right]\right\} \quad (32)$$

Equation (32) shows that the airfoil lift coefficient is an explicit function of the porosity of the porous plate. The lift coefficient increases as the porosity parameter decreases for a given sidewall displacement thickness. The lift coefficient is an implicit function of the plenum pressure through the displacement thickness δ^* in the quantity $\bar{\beta}$ [see Eq. (8)].

The individual effects of the pressure difference $p_\infty - p_p$ and the sidewall porosity coefficient P on the lift coefficient $\bar{C}_L$ can be seen from Eqs. (32) and (8). The effect of an increase in the pressure difference is a decrease in δ^* and, hence, $\bar{\beta}$ and a resultant increase in the lift coefficient. The effect of an increase in the sidewall porosity is more complicated. Assuming that the pressure difference $p_\infty - p_p$ is positive, the effect of an increase in the porosity coefficient is a decrease in the displacement thickness and, hence, a decrease in $\bar{\beta}$. This reduction in $\bar{\beta}$ tends to offset the reduction in the numerator of Eq. (32) caused by an increase in the porosity coefficient. However, it seems intuitive that an increase in porosity will result in a decrease in lift coefficient, because this increase permits more flow around the model tip and, hence, makes the model more three-dimensional.

The presence of the suction window also affects the drag measurement. It can be seen from Eq. (24) that beyond the window the dominant term in the first-order solution is a sink proportional to the pressure difference $p_\infty - p_p$. In other words, mass is removed at the window. Far from the model

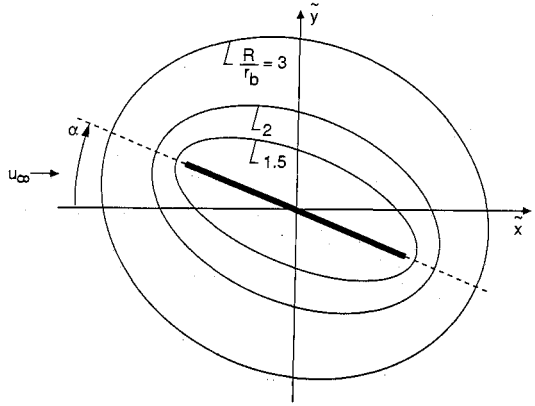

Fig. 6 Several suction windows in incompressible airfoil plane.

the drag can be represented as a source term. It follows that drag measurements with rakes located downstream of the model will be influenced by the presence of a suction window at the model station.

As already indicated, the suction window in the circle plane is circular and concentric to the circular body. As a result, the window in the incompressible airfoil plane is an ellipse with its axis aligned with the flat plate, and the window in the compressible airfoil plane is a flatter ellipse that is also aligned with the flat plate. The windows in the incompressible airfoil plane for several values of the parameter R/r_b are depicted in Fig. 6. These shapes, while not representing any actual suction windows, are not unrealistic in general appearance. As a result, the overall trends predicted in this article are qualitatively correct for two-dimensional wind tunnels with sidewall suction around the model.

Concluding Remarks

A closed-form analysis of flow in a two-dimensional subsonic wind tunnel that uses sidewall suction around the model to reduce sidewall boundary-layer effects is presented. The model problem that is treated involves a flat plate airfoil in a tunnel with a suction window shaped to permit an analytic solution. This solution shows that the lift coefficient depends explicitly on the porosity parameter of the suction window and implicitly on the suction pressure differential. For a given sidewall displacement thickness, the lift coefficient increases as the suction-window porosity decreases.

Although this solution applies only to a model problem, the more general problem of an arbitrary airfoil in a transonic wind tunnel with arbitrary suction-window geometry can be easily solved with state-of-the-art finite difference methods for two-dimensional transonic flow. The terms on the right side of Eq. (11), which account for the sidewall suction effect, are simply included in the appropriate computer program and evaluated at grid points adjacent to the suction window.

References

[1]Barnwell, R. W., "A Similarity Rule for Compressibility and Sidewall Boundary Layer Effects in Two-Dimensional Wind Tunnels," AIAA Paper 79-0108, Jan. 1979.

[2]Barnwell, R. W., "Similarity Rule for Sidewall Boundary-Layer Effect in Two-Dimensional Wind Tunnels," *AIAA Journal,* Vol. 18, No. 9, 1980, pp. 1149–1151.

[3]Bernard-Guelle, R., "Influence of Wind Tunnel Wall Boundary Layer on Two-Dimensional Transonic Tests," 12th Applied Aerodynamics Colloquium, ENSMA/CEAT, Poitiers, France, Nov. 5–7, 1975, ONERA, 1976, pp. 1–22; also available as NASA TT F-17255.

[4]Sewall, W, G., "Effects of Sidewall Boundary Layers in Two-Dimensional Subsonic and Transonic Wind Tunnels," *AIAA Journal,* Vol. 20, No. 9, 1982, pp. 1253–1256.

[5]Barnwell, R. W., and Sewall, W. G., "Similarity Rules for Effects of Sidewall Boundary Layer in Two-Dimensional Wind Tunnels," AGARD CP-335, May 1982, pp. 3.1–3.10.

[6]Murthy, A. V., "Effect of Aspect Ratio on Sidewall Boundary-Layer Influence in 2-D Airfoil Testing," NASA CR-4008, Sept. 1986.

[7]Su, Y. X., "Mechanism of Sidewall Effect Studied With Oil Flow Visualization," *AIAA Journal,* Vol. 27, No. 12, 1989, pp. 1828–1830.

[8]Ohman, L. H., and Brown, D., "The NAE High Reynolds Number 15 In. by 10 In. Two-Dimensional Test Facility, Pt. II: Results of Initial Calibration," Nuclear Regulartory Commission Lab. TR LTR-HA-4, National Research Council of Canada, Ottawa, Canada, Sept. 1970.